

Functional Quantitative and Qualitative Models for Quality Modeling in a Fused Deposition Modeling Process

Hongyue Sun¹, Member, IEEE, Prahalad K. Rao², Zhenyu (James) Kong³, Member, IEEE, Xinwei Deng, and Ran Jin⁴, Member, IEEE

Abstract—Additive manufacturing (AM) enables flexible part geometry and functionality, and reduces product development life cycle by direct layer-wise fabrication from CAD files. In the last decade, great achievements are made on AM materials, machines, processes, etc. However, the quality of the AM parts is still questionable for industrial specifications. On the one hand, AM part quality variables can be either quantitative, such as dimensional accuracy, or qualitative, such as binary indicators for voids, missing features, or surface roughness. On the other hand, both offline process setting variables and functional *in situ* process variables can be measured and modeled with both quantitative and qualitative (QQ) quality response variables. In this paper, the QQ quality response variables are modeled by offline process setting variables and *in situ* process variables via functional QQ models. The modeling of these *in situ* process variables provides the basis for real-time monitoring and control for AM processes. Simulation studies and experimental data from a fused deposition modeling process are performed to demonstrate the effectiveness of the proposed method.

Note to Practitioners—Additive manufacturing (AM) processes have attracted much attention and showed many advantages over the traditional subtractive manufacturing processes. However, the product quality issues make AM intractable for high-quality parts in industrial applications. This paper aims to address the quality issues by modeling both quantitative quality variables, such as dimensional accuracy, and qualitative quality variables, such as the binary (go/no-go) indicator for surface conditions. Both offline process setting variables and *in situ* process variables are used in the model as predictors. Such a model is important

Manuscript received October 1, 2016; revised June 5, 2017; accepted October 9, 2017. This work was supported by the National Science Foundation under Grant CMMI-1436592 and Grant CMMI-1435996. This paper was recommended for publication by Associate Editor Y. Chen and Editor C. C. L. Wang upon evaluation of the reviewers' comments. (Corresponding author: Hongyue Sun.)

H. Sun is with the Department of Industrial and Systems Engineering, University at Buffalo, Buffalo, NY 14260 USA (e-mail: hongyues@buffalo.edu).

P. K. Rao is with the Department of Mechanical and Materials Engineering, University of Nebraska–Lincoln, Lincoln, NE 68588 USA (e-mail: rao@unl.edu).

Z. Kong and R. Jin are with the Grado Department of Industrial and Systems Engineering, Virginia Tech, Blacksburg, VA 24061 USA (e-mail: zkong@vt.edu; jran5@vt.edu).

X. Deng is with the Department of Statistics, Virginia Tech, Blacksburg, VA 24061 USA (e-mail: xdeng@vt.edu).

This paper has supplementary downloadable multimedia material available at <http://ieeexplore.ieee.org> provided by the authors. The Supplementary Material includes the detailed simulation results for functional QQ models, and a comparison of number of part layers on the prediction performance. This material is 434 KB in size.

Color versions of one or more of the figures in this paper are available online at <http://ieeexplore.ieee.org>.

Digital Object Identifier 10.1109/TASE.2017.2763609

for systematically quality evaluation of AM parts, and provides the basis for future process monitoring and control. The merits of the proposed method are demonstrated with simulation studies and a case study in a fused deposition modeling process.

Index Terms—Additive manufacturing (AM), functional quantitative and qualitative (QQ) models, fused deposition modeling (FDM), *in situ* process variables, QQ responses.

I. INTRODUCTION

ADDITIVE manufacturing (AM) fabricates a part by printing materials layer by layer from a CAD file, thus enables flexible part geometry and reduces material wastes. Compared with the traditional subtractive manufacturing processes, AM can eliminate the time-consuming fixture and tool design steps. Therefore, it can significantly reduce the tooling and assembly cost, as well as the product development life cycle [1]–[3].

AM processes have shown their capability in various industries, such as aerospace, automobile, and healthcare [4]–[7]. For instance, maxillofacial, neurosurgical, and orthopedic medical parts were fabricated with stereolithography and fused deposition modeling (FDM) [4]. Commercial and military aircraft parts were fabricated with selective laser sintering [5]. However, most of these applications are still in the proof-of-concept phase, and several challenges need to be solved before the industrial applications of AM. Among these challenges, the product quality modeling and assurance is a key issue [1], [2].

We focus on the AM part quality modeling for a FDM AM process in this paper. A schematic of a desktop FDM printer is shown in Fig. 1 [8]. The process fabricates a part by successively printing layers of molten plastic filament on the substrate with the following procedures [7], [8]. First, the offline process setting variables (such as table temperature, layer thickness, etc.) are specified. Then, the filament heated over its glass transition temperature is extruded out of the extruder. The extruded material cools down and solidifies when it reaches the substrate. The extruder travels over the substrate to form the desired cross section profile for the current layer. Finally, the base plate moves down one layer, and the next layer is deposited. These successive layers solidify and bond together to form the part. In a FDM process, the part quality variables are affected by offline process setting variables, machine precision, material shrinkage, external environment,

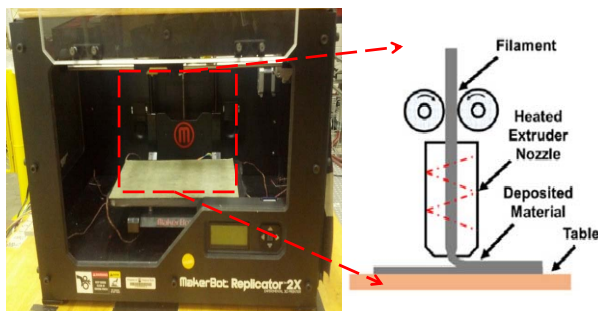


Fig. 1. Schematic illustration of a desktop FDM printer [8].

etc. These quality variables should be controlled to meet the design specifications.

To improve the part quality, the effects of various offline process setting variables, such as feed rate, flow rate, build orientation, layer thickness, extruder temperature, and raster angle on the part quality were studied [8], [9]. These quality variables can be quantitative or qualitative, such as dimensional accuracy [10]–[12], surface roughness [13]–[15], presence or number of voids [16]–[18], and presence of missing features [19], [20]. In most of the published works, these part quality variables were investigated separately based on the offline process setting variables. Limited attention was paid to the association of the quantitative and qualitative (QQ) types of part quality variables, and their relationships with the functional *in situ* process variables. Recently, it was demonstrated in a wafer lapping process that the joint modeling of QQ responses can improve the model prediction performance compared with separate modeling of each response [21]. But this paper is limited to model the *in situ* process variables. Rao *et al.* [8] developed a real-time sensing system for a FDM process. With the help of the sensing system, *in situ* process variables such as the vibration at the extruder and table, and the temperature at the melt pool and table can be collected [8]. It was shown that these *in situ* process variables were informative for predicting whether the FDM part will fail or not [8], [22]. Therefore, the *in situ* process variables should be considered in the FDM process modeling.

In this paper, we focus on the analysis of the association of the QQ quality variables in a FDM process. These quality variables are modeled by both offline process setting and *in situ* process variables via functional QQ models. The functional QQ models are widely applicable for the modeling of quantitative quality variables in AM, such as dimensional accuracy and mechanical property, and qualitative quality variables, such as surface roughness condition and missing features. The contributions of this paper mainly lie in the integration of *in situ* process variables into the QQ modeling framework. In addition, a hierarchical variable selection method [i.e., hierarchical nonnegative garrote (HNNG)] is used to identify not only which *in situ* process variables are significant, but also which features of these *in situ* process variables are significant in the modeling. In particular, HNNG rescales the initial model estimator (such as ridge estimator [23]) by nonnegative shrinkage factors, and uses two levels of constraints for the

variable selection (details to be discussed in Section III). HNNG was demonstrated in a logistic regression model for a binary defect indicator in a crystal growth process [23], and a linear regression model for a continuous comfort score in a vehicle ingress/egress comfort study [24]. However, HNNG was never reported for functional QQ models with both QQ responses and functional predictors. The unique features from the FDM process allow us to explore this new functional QQ modeling method.

The rest of this paper is organized as follows. The state-of-the-art for FDM quality improvements and the QQ responses modeling are reviewed in Section II. In Section III, the proposed functional QQ models are introduced. Simulation studies and a case study in a FDM process are used to demonstrate the effectiveness of the proposed method in Sections IV and V, respectively. Finally, summary and discussions are made in Section VI.

II. LITERATURE REVIEW

A. FDM Quality Improvements

In this section, we first review the studies on FDM part quality improvement, and then review the existing monitoring and control works for FDM processes.

Various quantitative quality response variables in FDM, such as mechanical property and dimensional accuracy, were studied. For instance, Fodran *et al.* [25] investigated the effect of air gap, layer thickness and filament width on tensile stress, tangent modulus, and part strength in qualitative experimental studies. Matas [26] proposed stiffness and strength models based on first principles. For dimensional accuracy, Sood *et al.* [10] used Taguchi methods for length, width, thickness, and diameter modeling, and found that different quality variables had different optimal process setting variables conditions. Boschetto and Bottini [12] proposed a geometrical model for FDM part irregularity and dimensional accuracy. Geometrical models were proposed for surface roughness characterization based on process setting variables [13], [14], [27]. Statistical models, such as analysis of variance, Taguchi methods and artificial neural network, were also applied for the quality modeling and improvements [11], [28], [29]. See also [15], [30], [31]. On the other hand, the qualitative quality response variables in FDM, such as presence or number of voids and missing features were also studied. For instance, Agarwala *et al.* [16] investigated various strategies, such as improving feed filament quality, optimizing build environment temperature, and adjusting process variables, to reduce or eliminate the presence of voids. Rodriguez *et al.* [17] concluded that the fiber gap and flow rate strongly affected the presence and number of voids. See also [19], [20], and a recent review in [9].

In this paper, we focus on the FDM part dimensional accuracy and surface roughness modeling. The dimensional accuracy can be measured by easily accessible tools such as calipers, while the surface roughness needed to be measured by contact or noncontact methods. In contact method (such as using a profilometer [12]), a stylus is dragged on the part surface, which may damage the part surface. Noncontact

method is nondestructive, but professional equipment, such as confocal microscopy, is needed. The public FDM users may not have access to professional noncontact equipment or even profilometer for surface roughness measurement. In addition, for the situation of *in situ* quality assessment of roughness, one cannot measure roughness based on profilometer or microscope during the printing. However, the users can easily observe part surface appearance, and provide a quick judgment of the surface roughness condition. Therefore, we treat surface roughness as a binary indicator based on the go/no-go judgment. Note that the proposed method can be generally applied to situations with QQ responses, and is not limited to the modeling of dimensional accuracy and surface roughness condition.

Recently, *in situ* process monitoring and control of AM processes attracted much attention [1]–[3], [32]. Until now, the majority of research and review for the monitoring and control were on metal-based AM processes [2], [3], [33]. For the FDM process, Dinwiddie *et al.* [34] used infrared cameras to monitor the temperature distribution of the extrusion process, where the temperature distribution was useful for modifying the part design. Kousiatza and Karalekas [35] embedded fiber Bragg grating sensors and thermocouples at different layers of a FDM part for *in situ* strain field and temperature profile monitoring, and showed that the sample location with regard to the building platform will significantly affect the strain and temperature. Rao *et al.* [8] built a real-time sensing system to capture the vibration, temperature, and video of the printing process. These *in situ* process variables can help monitor whether the part will fail or not [8], [22]. Tlegenov *et al.* [36] integrated the vibration measurement with physics-based dynamic model for FDM nozzle clog monitoring. Wu *et al.* [37] introduced the acoustic emission sensor for the FDM machine condition monitoring, and distinguished the normal, semiblock, block and run out of material conditions with the sensor signal. Shrinkage is a phenomenon that affects the dimensional accuracy of the FDM parts, and the offline shape shrinkage compensation was studied by various scholars to control the part shape to target [38]–[40].

The aforementioned works discovered many important facts about the quality variables in FDM, but failed to consider the association of both the QQ types of quality variables and their relationships with the process setting variables and *in situ* process variables systematically. QQ models are powerful in exploring the association of heterogeneous quality response variables, which are adopted in this paper.

B. QQ Responses Modeling

The QQ responses are widely encountered in biomedical, healthcare, and manufacturing systems [21], [41]–[43]. Traditionally, the QQ responses are modeled separately [44]–[48]. The separate modeling usually fails to keep track of the association of these heterogeneous responses, and may lead to inferior performance compared with joint modeling of QQ responses [21], [43].

The analysis of the QQ responses started with the correlation study [41], [49]. To model the QQ responses,

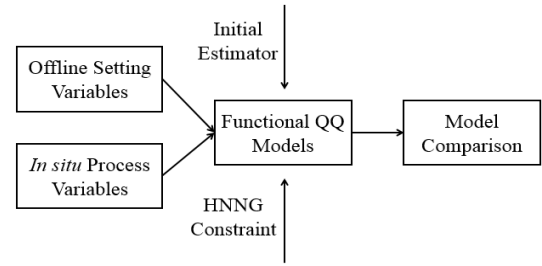


Fig. 2. Schematic of the proposed modeling framework.

Catalano and Ryan [50] used a continuous latent variable for a binary response, and assumed a joint Gaussian distribution for the latent variable and the continuous response. Fitzmaurice and Laird [51] incorporated covariates in a marginal model for the responses. The purposes of the above models were for independence test and model estimation, but not for variable selection to obtain a parsimonious and interpretable model.

Deng and Jin [21] proposed the QQ models for joint modeling of QQ responses by a constrained likelihood estimation, where the significant variables can be identified. Deng and Jin [21] applied the QQ models to a wafer lapping process where wafer total thickness variation was modeled as a quantitative response and site total indicator reading was modeled as a binary qualitative response. It was shown that joint modeling of the QQ responses can improve the model estimation and model prediction performance for the lapping process with scalar variables as model input, compared with the separate modeling approach [21]. In this paper, we generalize the QQ models to functional QQ models so that the functional *in situ* process variables can be modeled as predictors. Moreover, HNNG is used and generalized in the functional QQ models to select not only which functional variables, but also which features in the functional variables are important for the QQ responses [23], [24]. This hierarchical variable selection is enabled by two levels of constraints in HNNG to be discussed in Section III.

III. PROPOSED METHOD

A. Overview

The proposed method is illustrated in Fig. 2. The scalar offline process setting variables and functional *in situ* process variables are processed and used as input for the functional QQ models. In the functional QQ models, ridge regression estimator is used as initial estimator [23], and HNNG constraint enforces the model sparsity. Finally, the functional QQ models are compared with the benchmark models, where the QQ responses are modeled separately.

B. Functional QQ Models

Denote the data for the i th sample $\mathbf{x}_i = (\mathbf{x}_i^S; \mathbf{x}_i^F) = (x_{1,i}^S; \dots; x_{q,i}^S; \mathbf{x}_{1,i}^F; \dots; \mathbf{x}_{p,i}^F)$, where \mathbf{x}_i^S represents the scalar process setting variables and \mathbf{x}_i^F represents the functional *in*

situ process variables. $x_{k,i}^S$ is the k th process setting variable (such as extruder temperature in FDM), and $x_{j,i}^F$ is the j th *in situ* process variable (such as melt pool temperature in FDM), $k = 1, \dots, q$ and $j = 1, \dots, p$. “;” represents column-wise concatenation. We consider the problem with one quantitative response $y_i \in R$ (dimensional accuracy in FDM), and one qualitative (binary) response $z_i \in \{0, 1\}$ (surface roughness condition in FDM, where $z_i = 1$ represents bad surface roughness condition).

Following a similar spirit of QQ models for scalar variables [21], the functional QQ models use a functional logistic regression for the binary response z_i , and functional linear regressions for the continuous response y_i conditional on the binary response z_i

$$\begin{aligned} \text{logit}(E[z_i|x_i]) &= \log\left(\frac{p(x_i)}{1-p(x_i)}\right) = (x_i^S)^T \boldsymbol{\gamma}^S \\ &+ \int x_{1,i}^F(t) \tilde{\gamma}_1^F(t) dt + \dots + \int x_{p,i}^F(t) \tilde{\gamma}_p^F(t) dt \end{aligned} \quad (1)$$

$$\begin{aligned} (y_i|z_i = m) &= (x_i^S)^T \mathbf{b}^{S(m)} + \int x_{1,i}^F(t) \tilde{b}_1^F(t)^{(m)} dt + \dots \\ &+ \int x_{p,i}^F(t) \tilde{b}_p^F(t)^{(m)} dt + \varepsilon^{(m)}, \quad m = 0, 1 \end{aligned} \quad (2)$$

where $\boldsymbol{\gamma}^S = (\gamma_1^S, \dots, \gamma_q^S)^T$ and $\mathbf{b}^{S(m)} = (b_1^{S(m)}, \dots, b_q^{S(m)})^T$, $m = 0, 1$, is a vector of coefficients for scalar variables for the functional logistic regression and functional linear regressions, respectively. $\tilde{\gamma}_j^F(t)$ and $\tilde{b}_j^F(t)^{(m)}$, $j = 1, \dots, p$, $m = 0, 1$, is the coefficient for the j th functional variable in corresponding models. Assume the error distribution $\varepsilon^{(m)} \sim N(0, \sigma^2)$, $m = 0, 1$ [21].

The functional variables are measured over time, and usually have high dimensions. To address the high dimensionality issue, various basis expansion techniques, such as spline expansion, Fourier transform, and wavelet analysis are adopted [52]. We apply the basis expansion approach in this paper. Denote the orthogonal basis as $\boldsymbol{\theta}(t) = (\theta_1(t), \theta_2(t), \dots, \theta_K(t))^T$, we have $\tilde{\gamma}_j^F(t) = (\boldsymbol{\gamma}_j^F)^T \boldsymbol{\theta}(t)$, $\tilde{b}_j^F(t)^{(m)} = (\mathbf{b}_j^{F(m)})^T \boldsymbol{\theta}(t)$, $m = 0, 1$ after the basis expansion. $\boldsymbol{\gamma}_j^F$ and $\mathbf{b}_j^{F(m)}$, $m = 0, 1$, is a vector of K basis expansion coefficients for $\tilde{\gamma}_j^F(t)$ and $\tilde{b}_j^F(t)^{(m)}$, respectively. These K elements are from the same functional coefficients, and form a group [53]. Reorganizing (1) and (2), the proposed functional QQ models can be summarized with (see the Appendix for details)

$$z_i = \begin{cases} 1, & \text{with probability } p(\mathbb{x}_i) \\ 0, & \text{with probability } 1 - p(\mathbb{x}_i) \end{cases} \quad (3)$$

$$(y_i|z_i) \sim N(z_i \mathbb{x}_i^T \boldsymbol{\beta}^{(1)} + (1-z_i) \mathbb{x}_i^T \boldsymbol{\beta}^{(0)}, \sigma^2) \quad (4)$$

where $p(\mathbb{x}_i) = (\exp(\mathbb{x}_i^T \boldsymbol{\eta}) / (1 + \exp(\mathbb{x}_i^T \boldsymbol{\eta})))$, $\mathbb{x}_i = (x_i^T \boldsymbol{\phi})^T$, $\boldsymbol{\phi} = \text{diag}(I_{q \times q}, \boldsymbol{\theta}(t)^T, \dots, \boldsymbol{\theta}(t)^T)$, $\boldsymbol{\eta} = (\boldsymbol{\gamma}^S; \boldsymbol{\gamma}^F) = (\eta_1; \dots; \eta_q; \eta_{q+1}; \dots; \eta_{q+p})$, and $\boldsymbol{\gamma}^F = (\boldsymbol{\gamma}_1^F; \dots; \boldsymbol{\gamma}_p^F)$. $\boldsymbol{\beta}^{(m)}$, $m = 0, 1$ has similar structure to $\boldsymbol{\eta}$ (see the Appendix for details). Considering the group structure (i.e., the elements from the same functional coefficients after basis expansion

form a group), we have $q + p$ groups of coefficients. For q scalar variables (such as extruder temperature in FDM), the group size (i.e., number of coefficients in a group) is 1, and for the j th functional variables (such as melt pool temperature in FDM), the group size is P_{q+j} , $j = 1, \dots, p$. For FDM, the surface roughness condition can be modeled with (3), and the dimensional accuracy can be modeled with (4). If the coefficients $\boldsymbol{\beta}^{(1)}$ and $\boldsymbol{\beta}^{(0)}$ are identical both in terms of significant sets and values, i.e., the two linear models are the same no matter what the value of z_i is, the QQ responses are independent. Otherwise, the QQ responses are associated, and the joint modeling of the QQ responses has the potential to provide better prediction performance over separate modeling of the responses [21].

The model coefficients in (3) and (4) can be estimated with maximum likelihood estimation (MLE). However, the MLE is not feasible when the number of coefficients is larger than the sample size. Different penalties are proposed to learn a parsimonious and interpretable model [54]. When there are groups of coefficients, the group Lasso with $l_{1,2}$ penalty can be used for variable selection [53]. However, the $l_{1,2}$ penalty in group Lasso can only select a group of coefficients as a whole and cannot select individual coefficients in the group [23], [24]. To address the variable selection problem for selecting not only the groups but also the coefficients in the groups, the HNNG constraint is adopted in the functional QQ models. The model estimation can be solved by optimizing the objective function

$$\begin{aligned} \min & -2L(\boldsymbol{\eta}, \boldsymbol{\beta}^{(1)}, \boldsymbol{\beta}^{(0)}) \\ \text{s.t.} & (\varphi_{k,r})^{(m)} = (\varphi_{k,r})^{(m)} (\tilde{\beta}_{k,r})^{(m)}, \quad \eta_{k,r} = \tau_{k,r} \tilde{\eta}_{k,r}, \quad m = 0, 1 \\ & \sum_{k=1}^{P_r} w_r (\varphi_{k,r})^{(m)} \leq (\rho_r)^{(m)}, \quad \sum_{k=1}^{P_r} w_r \tau_{k,r} \leq \rho_r, \quad m = 0, 1 \\ & (\varphi_{k,r})^{(m)} \geq 0, \quad \tau_{k,r} \geq 0, \quad (\rho_r)^{(m)} \geq 0, \quad \rho_r \geq 0, \quad m = 0, 1 \\ & \sum_{r=1}^{p+q} ((\rho_r)^{(1)} + (\rho_r)^{(0)}) \leq M_1 \\ & \sum_{r=1}^{p+q} \rho_r \leq M_2 \end{aligned} \quad (5)$$

where $L(\boldsymbol{\eta}, \boldsymbol{\beta}^{(1)}, \boldsymbol{\beta}^{(0)}) = \log\{\prod_{i=1}^n f(y_i|z_i) f(z_i)\}$ is the log-likelihood function, $(\tilde{\beta}_{k,r})^{(m)}$ and $\tilde{\eta}_{k,r}$ are the initial estimators of the k th coefficient in the r th variable in functional linear regressions and functional logistic regression. The initial estimator is taken as ridge regression estimator [23]. $(\varphi_{k,r})^{(m)}$ and $\tau_{k,r}$ are nonnegative shrinkage factors for general variable selection [55]. The second line of the constraints controls the number of coefficients selected in each group of coefficients, where $w_r = \sqrt{P_r}$ is a weight factor proportional to the group size P_r of the r th group of coefficients. Adding such a weight factor will avoid the situation that the coefficients in a larger group is more likely to be selected compared with the coefficients in a smaller group [53], [55]. The hierarchical variable selection is fulfilled by the group level shrinkage factor $(\rho_r)^{(m)}$ or ρ_r , and the individual level shrinkage factor $(\varphi_{k,r})^{(m)}$ or $\tau_{k,r}$. If $(\rho_r)^{(m)}$ or ρ_r equals to zero, then the current group will not be selected. Otherwise, $(\varphi_{k,r})^{(m)}$ or $\tau_{k,r}$ controls whether a coefficient within a group will be selected.

The constraints in the last two lines control the total number of groups selected for the functional linear regressions (the model complexity for dimensional accuracy in FDM, controlled by M_1) and functional logistic regression (the model complexity for surface roughness condition in FDM, controlled by M_2), respectively. M_1 and M_2 can be selected by Bayesian information criterion, the prediction errors in cross validation (CV) or the prediction errors in validation data set [56].

It is worth pointing out that the unique formulation of the proposed functional QQ models over the QQ models for scalar variables [21] and the hierarchical variable selection method [23] includes the following.

- 1) The functional predictors (*in situ* process variables) are modeled for the first time in the QQ modeling framework.
- 2) The two tuning parameters M_1 and M_2 are used to separately control the complexity in the functional linear regressions and functional logistic regression.
- 3) The weight factor w_r is introduced to take the effect of group size into consideration during variable selection.

To optimize the objective function in (5) directly is a challenging task due to the complex likelihood function. Therefore, a quadratic approximation technique is used. The derivation follows the procedure of Deng and Jin [21]. After the quadratic approximation, the problem in (5) is simplified to a quadratic programming problem with guaranteed convergence [21]. In the following, both simulation studies and a case study in a FDM process are used to demonstrate the effectiveness of the proposed method.

IV. SIMULATION STUDIES

Denote $\mathbf{I}^{(1)}$ and $\mathbf{I}^{(0)}$ as the sets of significant coefficients in the underlying functional linear regressions, and \mathbf{I} as the set of significant coefficients in the underlying functional logistic regression. To evaluate the performance of the functional QQ models, four scenarios are considered in the simulation [21].

Scenario 1: the significant sets $\mathbf{I}^{(1)}$ and $\mathbf{I}^{(0)}$ are exactly the same, and the significant coefficients in $\beta^{(1)}$ and $\beta^{(0)}$ have similar values.

Scenario 2: the significant sets $\mathbf{I}^{(1)}$ and $\mathbf{I}^{(0)}$ do not overlap, but the significant coefficients in $\beta^{(1)}$ and $\beta^{(0)}$ have similar values.

Scenario 3: the significant sets $\mathbf{I}^{(1)}$ and $\mathbf{I}^{(0)}$ are exactly the same, but the significant coefficients in $\beta^{(1)}$ and $\beta^{(0)}$ have different values.

Scenario 4: the significant sets $\mathbf{I}^{(1)}$ and $\mathbf{I}^{(0)}$ do not overlap, and the significant coefficients in $\beta^{(1)}$ and $\beta^{(0)}$ have different values.

Furthermore, several factors are varied during the simulation data generation under each scenario: 1) the number of variables in the underlying models; 2) the correlation structure for the model input; and 3) the sparsity (percentage of significant coefficients) in the underlying models. See Table I for a summary of detailed settings of these factors and their meanings. Under each scenario, we have 16 combinations of simulation settings.

TABLE I
SIMULATION SETTING

Factors	Levels	Meanings
Number of variables	1: $p = 2, q = 4$ 2: $p = 4, q = 8$	p : number of functional variables; q : number of scalar variables.
Correlation structure	1: $\rho_1 = 0, \rho_2 = 0$ 2: $\rho_1 = 0.6, \rho_2 = 0$ 3: $\rho_1 = 0, \rho_2 = 0.3$ 4: $\rho_1 = 0.6, \rho_2 = 0.3$	ρ_1 : within group correlation coefficient; ρ_2 : among group correlation coefficient.
Sparsity	1: $S = 0.2$ 2: $S = 0.4$	Percentage of significant coefficients in the underlying models.

For each simulation setting, the data are generated from (3) and (4). Specifically, $\mathbf{x}_i \sim N(\boldsymbol{\mu}, \Sigma)$, where the mean vector $\boldsymbol{\mu} = (\mu_1; \dots; \mu_q; \boldsymbol{\mu}_{q+1}; \dots; \boldsymbol{\mu}_{q+p})$, $\mu_j, j = 1, \dots, q$ is the mean for the j th scalar variable, and $\boldsymbol{\mu}_{q+k}$ is the mean for the k th functional variable. The number of coefficients in each functional variable is set to be 10. Here, $\boldsymbol{\mu}$ is set to be a zero vector. The covariance matrix $\Sigma = \text{diag}(\Sigma^S, \Sigma^F)$, $\Sigma^S = I_{q \times q}$ is the covariance matrix for the scalar variables

$$\Sigma^F = \begin{pmatrix} \Sigma_{11} & \dots & \Sigma_{1p} \\ \vdots & \ddots & \vdots \\ \Sigma_{p1} & \dots & \Sigma_{pp} \end{pmatrix}$$

is the covariance matrix for the functional variables

$$\Sigma_{rr} = \begin{bmatrix} 1 & \rho_1^{|i-j|} & \dots & \rho_1^{|i-j|} \\ \rho_1^{|i-j|} & 1 & \dots & \rho_1^{|i-j|} \\ \dots & \dots & \dots & \dots \\ \rho_1^{|i-j|} & \rho_1^{|i-j|} & \dots & 1 \end{bmatrix}_{P_r \times P_r}$$

is the within group covariance matrix for coefficients in the r th functional variable

$$\Sigma_{rs} = \begin{bmatrix} \rho_2 & \rho_2^{|i-j|+1} & \dots & \rho_2^{|i-j|+1} \\ \rho_2^{|i-j|+1} & \rho_2 & \dots & \rho_2^{|i-j|+1} \\ \dots & \dots & \dots & \dots \\ \rho_2^{|i-j|+1} & \rho_2^{|i-j|+1} & \dots & \rho_2 \end{bmatrix}_{P_r \times P_s}$$

is the among group covariance matrix for coefficients in the r th and s th functional variable. Three data sets, training, validation and testing data sets of sample sizes $n_{tr} = 100$, $n_{va} = 100$, and $n_{te} = 200$ are generated for each setting. Note that one can also generate the simulation data by first generating the functional variables, and then using basis expansion to decompose the functional variables to form x_i , but the nature of the problem will not change.

The model coefficients are generated as follows. For scenarios 1 and 2, $\beta_0^{(1)} \sim N(\boldsymbol{\mu}', I)$, $\boldsymbol{\mu}'$ has the same structure as $\boldsymbol{\mu}$. The scalar variables' coefficients in $\boldsymbol{\mu}'$ have mean 2, and the functional variables' coefficients in $\boldsymbol{\mu}'$ have mean 1, where $\mathbf{1}$ is a vector composed of 1s. I is an identity matrix. The coefficients in $\beta_0^{(0)}$ is generated by adding a small perturbation that follows $N(0, 0.1^2)$ to coefficients in $\beta_0^{(1)}$. For scenarios 3 and 4, $\beta_0^{(1)}$ and $\beta_0^{(0)}$ are generated independently of $N(\boldsymbol{\mu}', I)$ and $N(\boldsymbol{\mu}' + 3, I)$, respectively. For all scenarios, $\eta_0 \sim (1/2)N(\boldsymbol{\mu}', I)$. The elements in the significant sets $\mathbf{I}^{(1)}$

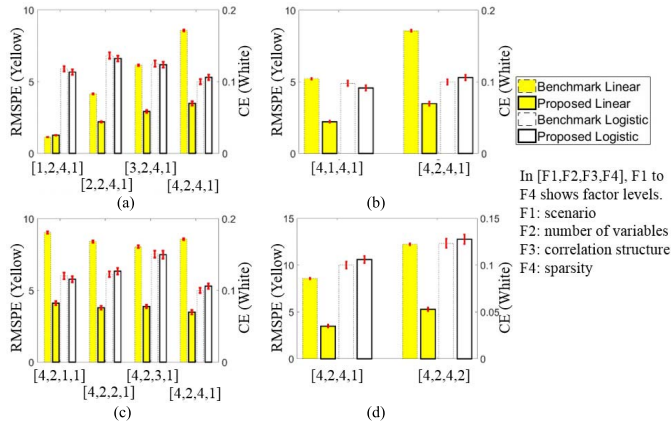


Fig. 3. Summary of representative simulation average testing RMSPE (yellow) for the quantitative response and CE (white) for the qualitative response. The vertical line on each bar (red) shows the standard error of RMSPE or CE over 50 replications. (a) Compare four scenarios. (b) Compare number of variables. (c) Compare correlation structure. (d) Compare density.

and $\mathbf{I}^{(0)}$ and \mathbf{I} take binary values, and are randomly generated according to the conditions in scenarios 1–4. Finally, $\boldsymbol{\beta}^{(1)}$, $\boldsymbol{\beta}^{(0)}$ and $\boldsymbol{\eta}$ are obtained by $\boldsymbol{\beta}^{(1)} = \boldsymbol{\beta}_0^{(1)} \cdot \mathbf{I}^{(1)}$, $\boldsymbol{\beta}^{(0)} = \boldsymbol{\beta}_0^{(0)} \cdot \mathbf{I}^{(0)}$, and $\boldsymbol{\eta} = \boldsymbol{\eta}_0 \cdot \mathbf{I}$, where represents elementwise multiplication. Finally, $\varepsilon^{(m)} \sim N(0, 1)$, $m = 0, 1$.

We compare the proposed functional QQ models with benchmark models, where l_1 penalized functional linear regressions and an l_1 penalized functional logistic regression are separately used for modeling the QQ responses [57]. For each simulation setting, 50 replications are performed. In each replication, the training data set is used for model estimation, the validation data set is used for tuning parameters selection, and the model prediction performance is evaluated with the testing data set. Specifically, the tuning parameters that yield the smallest prediction errors in the validation data set are selected for model prediction.

Fig. 3 shows comparisons of some representative average testing root-mean-square prediction errors (RMSPE) for the quantitative response and classification errors (CE) for the qualitative response over 50 replications, and the standard errors over these replications are shown in the red error bar. The smaller the errors, the better the models perform. In each plot of Fig. 3, the left vertical axis shows the scale for average RMSPE (yellow), the right vertical axis shows the scale for average CE (white), and the horizontal axis shows different simulation settings. These simulation settings are indexed by the numbers in the parenthesis (see Table I for detailed values and meanings of these numbers). For instance, [1, 1, 4, 2] represents the current simulation setting is for the first scenario, the first number of variables level ($p = 2, q = 4$), the fourth correlation structure level ($\rho_1 = 0.6, \rho_2 = 0.3$), and the second sparsity level ($S = 0.4$). A list of average testing RMSPE and CE along their standard errors over all simulation settings are provided in Table S-I in the supplemental materials.

The major conclusions from the simulation are the following:

- 1) For scenario 1 (at fixed levels for other factors), the benchmark models have comparable prediction

performance with the functional QQ models [the leftmost setting in Fig. 3(a)].

- 2) For scenarios 2–4 (at fixed levels for other factors), the functional QQ models perform better than benchmark models for the quantitative response prediction, and the two models are comparable for the qualitative response prediction [the last three settings in Fig. 3(a)].
- 3) When the number of variables or the proportion of significant coefficients in the underlying models increases, both the RMSPE in the proposed and benchmark models increase [from the setting in the left to the setting in the right in Fig. 3(b) and (d)]. And the advantage of the proposed models over benchmark models becomes more obvious under the above situations.

The functional QQ models perform well under scenarios 2–4 since the underlying models for the quantitative response at different conditions of the qualitative response are different, and the association of the QQ responses can be borrowed to enhance the model performance.

Fig. 4 shows comparisons of some representative variable selection accuracy over 50 replications, where a variable is treated important if it is selected in more than half of the replications (i.e., 25 replications). The variable selection accuracy is calculated as the proportion of significant coefficients in the underlying model being selected or insignificant coefficients in the underlying model being eliminated. For benchmark linear regression, we compare the estimated model with the underlying $m = 1$ and $m = 0$ linear models to obtain the accuracy for “Benchmark Linear $m = 1$ ” and “Benchmark Linear $m = 0$,” respectively. The vertical axis in each plot of Fig. 4 represents the variable selection accuracy, and the horizontal axis has the same meaning as those in Fig. 3. A list of overall variable selection accuracy, true positive rate (proportion of significant coefficients in the underlying model being selected) and true negative rate (proportion of insignificant coefficients in the underlying model being eliminated) over all simulation settings are provided in Tables S-II–S-IV in the supplemental materials. For the variable selection accuracy, the proposed models have better variable selection accuracy than benchmark models under scenarios 2–4 [the last three settings in Fig. 4(a)]. The variable selection accuracy (especially in the linear $m = 1$ model) tends to decrease when the number of variables or the proportion of significant coefficients in the underlying models increases [from the setting in the left to the setting in the right in Fig. 4(b) and (d)], which is consistent with the results in Fig. 3(b) and (d). The advantage of the proposed models is more obvious for these situations.

V. CASE STUDY

The proposed functional QQ models are applied to a FDM process. In this process, a part modified from National Aerospace Standard (NAS) 979 standard testing part [Fig. 5(a)] is printed with Acrylonitrile Butadiene Styrene material by MakerBot Replicator 2X [8]. During the experiment, three factors are varied: feed/flow ratio, layer thickness, and extruder temperature [8]. Other process variables, such as extruder travel path, filament diameter, etc., are kept constant.

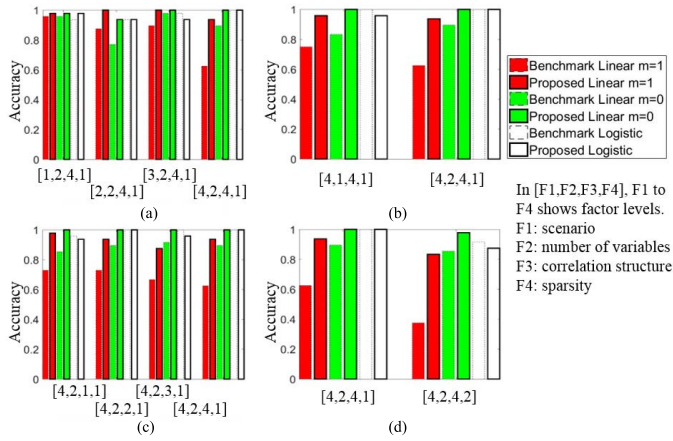


Fig. 4. Summary of representative simulation variable selection accuracy comparison. (a) Compare four scenarios. (b) Compare number of variables. (c) Compare correlation structure. (d) Compare density.

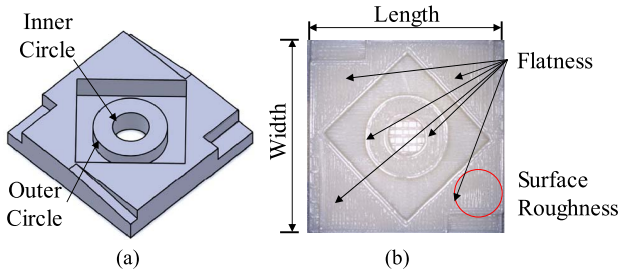


Fig. 5. (a) FDM test part modified from NAS 979 standard part [8]. (b) FDM printed part and representative quality variables.

In total, we have 44 successfully printed parts, where *in situ* process variables are collected from the sensor network [8]. After the parts are printed [Fig. 5(b)], their dimensional accuracy is inspected by the coordinate measurement machine. The dimensional accuracy variables measured include (Fig. 5): part width, part length, diameter of the outer circle, top plane flatness, outer circle roundness, innercircle roundness, concentric of the two circles, coaxial of the two circles, and run-out cylindricity of the outer circle. The surface roughness (go/no-go) is judged by domain experts, where the “no-go” samples are indexed by 1 and “go” samples are indexed by 0.

Since the part roughness judgment is only related to the surface and the dimensional accuracy is related to all layers but mainly determined by the layers close by the surface, we extract the segment of the *in situ* process variables that corresponded to the top several layers for the quality modeling. Specifically, the segments for the top three layers are extracted in this paper, where the data for different layers are separated based on the part g-code. If the printing quality in between the layers can be measured, the corresponding *in situ* measurements for the quality variable can be extracted and used for the modeling. Fig. 6(a)–(c) shows the sensor system, and Fig. 6(d) shows an example of the three axes vibration signals at extruder and table, and temperature signals at melt pool and table. See the details of the sensor type, placement, etc., in [8]. In particular, The melt pool temperature is measured with IR temperature sensor (Exergen UIRT/C.4-440F) located at the extruder head pointing toward the melt pool [Fig. 6(a)], the vibration data are measured with tri-axis

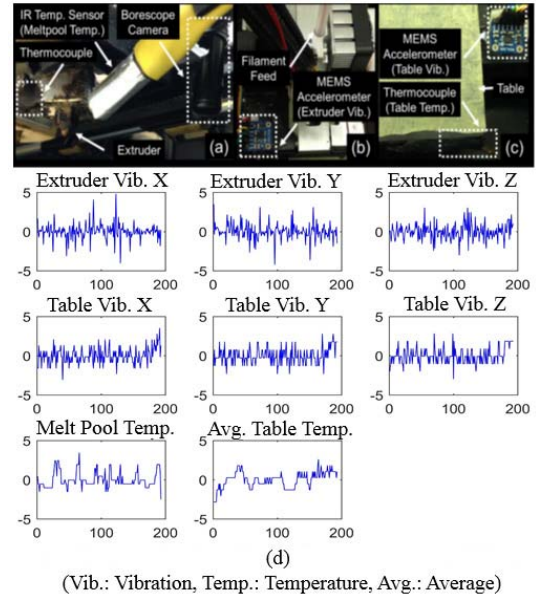


Fig. 6. (a)–(c) Sensor placement in the sensor network [8]. (d) Example of standardized *in situ* process variables.

accelerometer (Analog Devices ADXL335) located at extruder arm and table respectively for extruder vibration and table vibration measurement [Fig. 6(b) and (c)], and the table temperature is measured with thermocouples (Omega 5TC-GG-K-20-36) located at four corners of the printer table [Fig. 6(c)]. The vibration and table temperature signals are measured at a sampling frequency of ~ 2.5 Hz, and the melt pool temperature signal is measured at a sampling frequency of 1 Hz. All signals are synchronized to the same frequency of 1 Hz in the analysis. Such a sensor selection and frequency combination has shown to be effective to reflect the FDM process condition [8], [22]. In this paper, the qualitative engineering knowledge on the potential important variables for product quality is used for the sensor selection and feature generation. The quantitative engineering knowledge can also be used to facilitate the analysis, but such quantitative knowledge is not well established, and is beyond the scope of this paper. In each Fig. 6(d), the vertical axis shows the standardized signal values, and the horizontal axis shows the sample points. To investigate the effect of number of layers in the analysis, we vary the total number of layers (segmented based on g-code) used in the modeling. The corresponding results are reported in the supplemental materials. For our particular case, the top three layers yield good model performance since they are related to the surface quality. Note that the extraction of segments of *in situ* process variables in the quality modeling depends on the part quality feature under study. The part design file and g-code can be used for the alignment of quality feature of interest with corresponding segments of *in situ* process variables. The extraction of segments of *in situ* process variables based on a particular quality feature will be investigated in the future work.

For extruder and table vibration, the power spectrum density (PSD) is calculated based on the x -, y -, and z -axes vibration measurement [58]. The PSD of vibration signal

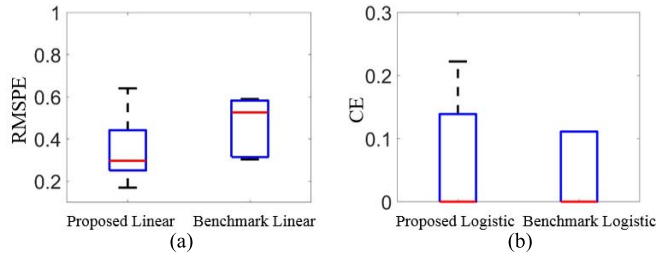


Fig. 7. Boxplots of testing. (a) RMSPE for quantitative response. (b) CE for the quantitative response.

is widely used for machine condition monitoring and fault diagnosis [58]. The PSD of three axes is calculated as one variable since the vibration in all axes tends to affect the part quality, and we are interested in the effects of the entire vibration at the extruder and at the table on the part quality. The hypothesis to be tested is that the PSD values are important, which means the larger vibration in local area would affect the product quality. As a result, we have 86 features for extruder and table vibration, separately. For melt pool temperature and average table temperature, 56 features are generated with the spline basis expansion. The PSD and basis expansion are used instead of synthetic descriptors (such as mean and standard deviation), since synthetic descriptors will incur much information loss and there is no engineering perception to indicator which synthetic descriptors to be used. The process setting variables and their two-way interactions are also considered, which include six features. In total, we have 290 features as model inputs. We take the first principle component (PC) of the dimensional accuracy variables as the quantitative response, and the surface roughness condition as the qualitative (binary) response. The first PC is used as a composite quality indicator in this paper to represent the overall part dimensional accuracy, and functional QQ models with multiple quantitative responses will be considered in the future work.

We use two levels of fivefold CV for tuning parameters selection and model evaluation, separately. fivefold CV is used since the sample size in the case study is limited for generating a validation data set for tuning parameters selection. Specifically, we first divide the samples approximately equally into fivefolds (first level CV), and select four of them as training data set. During the model fitting, the selected training data set is further divided approximately equally into fivefolds (second level CV). The tuning parameters are selected by the second level CV, i.e., M_1 and M_2 yielding the smallest average testing errors in the second level CV are selected. The model performance is evaluated by the first level CV. The boxplots of the testing RMSPE and CE for the proposed models and benchmark models under the fivefold CV are shown in Fig. 7. From Fig. 7, the functional QQ models have better prediction performance than the benchmark models for the quantitative response, and the two approaches have comparable performance for the qualitative response prediction. This is because the quantitative dimensional accuracy is modeled conditional on the qualitative surface roughness condition, and

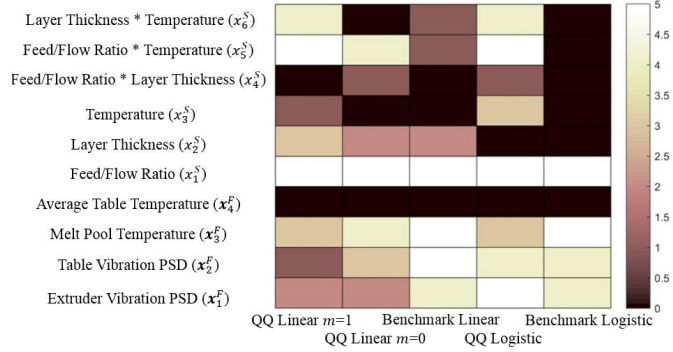


Fig. 8. Number of times a variable being selected over fivefold CV.

the functional linear regressions for the quantitative dimensional accuracy under different surface roughness condition are different (the first two columns in Fig. 8). Therefore, the functional QQ models are valuable for the QQ responses modeling in the FDM process.

Furthermore, a summary of the selected variables over the fivefold CV (first level CV) is shown in Fig. 8. In Fig. 8, an *in situ* process variable is regarded as selected if one or more of its element is selected. Each column in Fig. 8 represents a model, and each row represents a variable or two-way interaction between variables. The intensity (color bar) in Fig. 8 shows the number of times a variable being selected in the fivefold CV. From Fig. 8, both offline process setting variables and *in situ* process variables are important for the quality modeling, and the two linear models under the different surface roughness conditions are different. Note that the conditional relationships between the qualitative response (surface roughness condition) and quantitative response (dimensional accuracy) in (6) and (7) show the association among the QQ responses, but not causal relationships. The functional QQ models can enhance the prediction performance for the quantitative response based on this association [Fig. 7(a)], compared with the benchmark separate modeling of QQ responses. In particular, the feed/flow ratio governing the ratio of how fast the nozzle travels and how fast the material is extruded from the nozzle is very important for the part quality. The *in situ* process variables extruder vibration, table vibration, and melt pool temperature are important for modeling the dimensional accuracy and surface roughness condition (as shown in the last three rows in Fig. 8). This is because the changes in extruder vibration, table vibration, and temperature in the melt pool area are informative for the process condition. Moreover, the functional QQ models in the last CV fold for dimensional accuracy with the surface roughness at bad condition ($m = 1$) and at good condition ($m = 0$), and for surface roughness condition are shown in (6)–(8), respectively. The variable names in (6)–(8) are available in Fig. 8. For instance, $x_{3,55}^F$ refers to the 55th elements in the melt pool temperature, and x_1^S refers to feed/flow ratio

$$(y_i | z_i = 1) = -0.038x_{3,55}^F - 0.912x_1^S + 0.382x_2^S - 0.149x_5^S + 0.005x_6^S \quad (6)$$

$$(y_i|z_i=0) = 0.012x_{1,37}^F + 0.092x_{2,37}^F + 0.007x_{2,82}^F + 0.050x_{3,40}^F - 0.864x_1^S + 0.050x_2^S - 0.035x_5^S \quad (7)$$

$$\begin{aligned} \text{logit}(E[z_i|x_i]) = & -1.328 - 0.291x_{1,15}^F + 0.754x_{1,53}^F \\ & + 0.692x_{2,3}^F + 0.240x_{2,20}^F + 0.488x_{3,40}^F \\ & - 1.283x_1^S + 0.378x_3^S - 0.142x_4^S - 1.202x_5^S \\ & + 0.671x_6^S. \end{aligned} \quad (8)$$

These equations are helpful for the AM processes quality monitoring and control. For instance, one can monitor whether the surface roughness or dimensional accuracy is at a desired condition based on the offline setting variables and *in situ* process variables by control charts [59], [60]. Equations (6) and (7) can also be used for the dimensional accuracy control [61]. Note that the model parameters will vary for different applications, and need to be refitted for other machines and applications.

VI. SUMMARY AND DISCUSSION

AM is a promising manufacturing process to produce flexible part, reduce material waste, and product development life cycle. In the past decade, both industry and academia have investigated intensively to help with the wide deployment of AM applications. More investigations are still needed for quality control and assurance in AM processes.

In this paper, we investigate the heterogeneous types of quality responses in an FDM AM process. The dimensional accuracy (quantitative response) and surface roughness condition (qualitative response) are jointly modeled with both offline process setting variables and *in situ* process variables. Functional QQ models are newly proposed to fulfill the above task. It is demonstrated that the product quality responses can be better predicted by jointly considering the QQ responses. The offline process setting variables feed/flow ratio, layer thickness, extruder temperature and their two-way interactions, and the *in situ* process variables extruder vibration, table vibration, and melt pool temperature are important for the part quality modeling. The functional QQ models are also evaluated in the simulation studies, and yield better prediction and variable selection results as long as the underlying linear models vary with different values of the qualitative response. The functional QQ models provide a tool to access the part quality and serve the basis for future QQ responses monitoring and control.

Several directions can be pursued in the future work. First, functional QQ models can be generalized so that multiple dimensional accuracy responses can be jointly modeled. In addition, multiple qualitative responses, such as number of voids, missing features will also be included in the functional QQ modeling framework. Second, the spatial response for complex geometry, such as point cloud data, and spatial input, such as process video and infrared camera data, will be handled. Finally, the estimated QQ models will be used for process monitoring and control.

APPENDIX

After basis expansion, (1) and (2) become

$$\begin{aligned} \text{logit}(E[z_i|x_i]) = \log\left(\frac{p(x_i)}{1-p(x_i)}\right) = & (x_i^S)^T \boldsymbol{\gamma}^S \\ & + \sum_{j=1}^p \sum_{t \in \Psi} x_{j,i}^F(t) (\boldsymbol{\gamma}_j^F)^T \boldsymbol{\theta}(t) \end{aligned} \quad (A1)$$

$$\begin{aligned} (y_i|z_i=m) = & (x_i^S)^T \boldsymbol{b}^{S(m)} + \sum_{j=1}^p \sum_{t \in \Psi} x_{j,i}^F(t) (\boldsymbol{b}_j^{F(m)})^T \boldsymbol{\theta}(t) \\ & + \varepsilon^{(m)}, \quad m = 0, 1 \end{aligned} \quad (A2)$$

where Ψ is the time continuum of the corresponding functional variables. Reorganizing the above expression

$$\log\left(\frac{p(x_i)}{1-p(x_i)}\right) = \boldsymbol{x}_i^T \boldsymbol{\phi} \boldsymbol{\eta} = \boldsymbol{x}_i^T \boldsymbol{\eta} \quad (A3)$$

$$(y_i|z_i=m) = \boldsymbol{x}_i^T \boldsymbol{\beta}^{(m)} + \varepsilon^{(m)}, \quad m = 0, 1 \quad (A4)$$

where $\boldsymbol{\phi} = \text{diag}(I_{q \times q}, \boldsymbol{\theta}^T, \dots, \boldsymbol{\theta}(t)^T)$, $\boldsymbol{x}_i = (x_i^T \boldsymbol{\phi})^T$, $\boldsymbol{\eta} = (\boldsymbol{\gamma}^S; \boldsymbol{\gamma}^F) = (\eta_1; \dots; \eta_q; \boldsymbol{\eta}_{q+1}; \dots; \boldsymbol{\eta}_{q+p})$, and $\boldsymbol{\gamma}^F = (\boldsymbol{\gamma}_1^F; \dots; \boldsymbol{\gamma}_p^F)$. Similarly, $\boldsymbol{\beta}^{(m)} = (\boldsymbol{b}^{S(m)}; \boldsymbol{b}^{F(m)}) = (\beta_1^{(m)}; \dots; \beta_q^{(m)}; \boldsymbol{\beta}_{q+1}^{(m)}; \dots; \boldsymbol{\beta}_{q+p}^{(m)})$ and $\boldsymbol{b}^{F(m)} = (\boldsymbol{b}_1^{F(m)}; \dots; \boldsymbol{b}_p^{F(m)})$, $m = 0, 1$. Note that the vectors of coefficients $\boldsymbol{\eta}_{q+j}$ and $\boldsymbol{\beta}_{q+j}^{(m)}$, $m = 0, 1$, for the functional variables have P_{q+j} elements to form a group [53].

ACKNOWLEDGMENT

The authors would like to thank undergraduate students including W. Andersen, N. Bambino, H. Lee, Y. Li, A. Park, D. Roberson, J. Snyder, D. Valdez, and H. Zhao and master student A. Kar at Virginia Tech, Blacksburg, VA, USA, for their assistance in data collection.

REFERENCES

- [1] J. Scott, N. Gupta, C. Weber, S. Newsome, T. Wohlers, and T. Caffrey, "Additive manufacturing: Status and opportunities," *Sci. Technol. Policy Inst.*, pp. 1–29, Mar. 2012.
- [2] G. Tapia and A. Elwany, "A review on process monitoring and control in metal-based additive manufacturing," *J. Manuf. Sci. Eng.*, vol. 136, no. 6, p. 060801, 2014.
- [3] W. E. Frazier, "Metal additive manufacturing: A review," *J. Mater. Eng. Perform.*, vol. 23, no. 6, pp. 1917–1928, 2014.
- [4] J. Winder and R. Bibb, "Medical rapid prototyping technologies: State of the art and current limitations for application in oral and maxillofacial surgery," *J. Oral Maxillofacial Surg.*, vol. 63, no. 7, pp. 1006–1015, 2005.
- [5] B. Lyons, "Additive manufacturing in aerospace: Examples and research outlook," *Bridge*, vol. 44, no. 3, pp. 13–19, 2014.
- [6] B. N. Johnson, "3D printed nervous system on a chip," *Lab Chip*, vol. 16, no. 8, pp. 1393–1400, 2016.
- [7] T. Campbell, C. Williams, O. Ivanova, and B. Garrett, "Could 3D printing change the world," Technol., Potential, Implications Addit. Manuf., Atlantic Council, Washington, DC, USA, Tech. Rep. 17, Oct. 2011.
- [8] P. K. Rao, J. P. Liu, D. Roberson, Z. J. Kong, and C. Williams, "Online real-time quality monitoring in additive manufacturing processes using heterogeneous sensors," *J. Manuf. Sci. Eng.*, vol. 137, no. 6, p. 061007, 2015.
- [9] A. Garg, K. Tai, and M. M. Savalani, "State-of-the-art in empirical modelling of rapid prototyping processes," *Rapid Prototyping J.*, vol. 20, no. 2, pp. 164–178, 2014.
- [10] A. K. Sood, R. K. Ohdar, and S. S. Mahapatra, "Improving dimensional accuracy of fused deposition modelling processed part using grey taguchi method," *Mater. Des.*, vol. 30, no. 10, pp. 4243–4252, 2009.

- [11] I. Gajdoš and J. Slota, "Influence of printing conditions on structure in FDM prototypes," *Tech. Gazette*, vol. 20, no. 2, pp. 231–236, 2013.
- [12] A. Boschetto and L. Bottini, "Accuracy prediction in fused deposition modeling," *Int. J. Adv. Manuf. Technol.*, vol. 73, pp. 913–928, Jul. 2014.
- [13] D. Ahn, H. Kim, and S. Lee, "Surface roughness prediction using measured data and interpolation in layered manufacturing," *J. Mater. Process. Technol.*, vol. 209, no. 2, pp. 664–671, 2009.
- [14] C. J. L. Pérez, J. V. Calvet, and M. A. Sebastián Pérez, "Geometric roughness analysis in solid free-form manufacturing processes," *J. Mater. Process. Technol.*, vol. 119, nos. 1–3, pp. 52–57, 2001.
- [15] A. Boschetto, V. Giordano, and F. Veniali, "Modelling micro geometrical profiles in fused deposition process," *Int. J. Adv. Manuf. Technol.*, vol. 61, nos. 9–12, pp. 945–956, 2012.
- [16] M. K. Agarwala, V. R. Jamalabad, N. A. Langrana, A. Safari, P. J. Whalen, and S. C. Danforth, "Structural quality of parts processed by fused deposition," *Rapid Prototyping J.*, vol. 2, no. 4, pp. 4–19, 1996.
- [17] J. F. Rodriguez, J. P. Thomas, and J. E. Renaud, "Characterization of the mesostructure of fused-deposition acrylonitrile-butadiene-styrene materials," *Rapid Prototyping J.*, vol. 6, no. 3, pp. 175–186, 2000.
- [18] R. K. Chen, T. T. Lo, L. Chen, and A. J. Shih, "Nano-CT characterization of structural voids and air bubbles in fused deposition modeling for additive manufacturing," in *Proc. ASME Int. Manuf. Sci. Eng. Conf.*, Charlotte, NC, USA, Jun. 2015, p. V001T02A071.
- [19] W. Cheng, J. Y. H. Fuh, A. Y. C. Nee, Y. S. Wong, H. T. Loh, and T. Miyazawa, "Multi-objective optimization of part-building orientation in stereolithography," *Rapid Prototyping J.*, vol. 1, no. 4, pp. 12–23, 1995.
- [20] F. Xu, Y. S. Wong, H. T. Loh, J. Y. H. Fuh, and T. Miyazawa, "Optimal orientation with variable slicing in stereolithography," *Rapid Prototyping J.*, vol. 3, no. 3, pp. 76–88, 1997.
- [21] X. Deng and R. Jin, "QQ models: Joint modeling for quantitative and qualitative quality responses in manufacturing systems," *Technometrics*, vol. 57, no. 3, pp. 320–331, 2015.
- [22] K. Bastani, P. K. Rao, and Z. Kong, "An online sparse estimation-based classification approach for real-time monitoring in advanced manufacturing processes from heterogeneous sensor data," *IIE Trans.*, vol. 48, no. 7, pp. 579–598, 2016.
- [23] H. Sun, X. Deng, K. Wang, and R. Jin, "Logistic regression for crystal growth process modeling through hierarchical nonnegative garrote-based variable selection," *IIE Trans.*, vol. 48, no. 8, pp. 787–796, 2016.
- [24] K. Paynabar, J. Jin, and M. P. Reed, "Informative sensor and feature selection via hierarchical nonnegative garrote," *Technometrics*, vol. 57, no. 4, pp. 514–523, 2015.
- [25] E. Fodran, M. Koch, and U. Menon, "Mechanical and dimensional characteristics of fused deposition modeling build styles," in *Proc. Solid Freeform Fabrication*, 1996, pp. 419–442.
- [26] J. F. R. Matas, "Modeling the mechanical behavior of fused deposition acrylonitrile-butadiene-styrene polymer components," Ph.D. dissertation, Mech. Eng., Univ. Notre Dame, Notre Dame, IN, USA, 1999.
- [27] D. Ahn, J. H. Kweon, S. Kwon, J. Song, and S. Lee, "Representation of surface roughness in fused deposition modeling," *J. Mater. Process. Technol.*, vol. 209, no. 15, pp. 5593–5600, 2009.
- [28] B. H. Lee, J. Abdullah, and Z. A. Khan, "Optimization of rapid prototyping parameters for production of flexible ABS object," *J. Mater. Process. Technol.*, vol. 169, no. 1, pp. 54–61, 2005.
- [29] A. Sood, R. K. Ohdar, and S. S. Mahapatra, "A hybrid ANN-BFOA approach for optimization of FDM process parameters," in *Swarm, Evolutionary, and Memetic Computing* (Lecture Notes in Computer Science), B. Panigrahi, S. Das, P. Suganthan and S. Dash, Eds. Berlin, Germany: Springer, 2010, pp. 396–403.
- [30] A. Boschetto, V. Giordano, and F. Veniali, "Surface roughness prediction in fused deposition modelling by neural networks," *Int. J. Adv. Manuf. Technol.*, vol. 67, nos. 9–12, pp. 2727–2742, 2013.
- [31] R. Anitha, S. Arunachalam, and P. Radhakrishnan, "Critical parameters influencing the quality of prototypes in fused deposition modelling," *J. Mater. Process. Technol.*, vol. 118, nos. 1–3, pp. 385–388, 2001.
- [32] M. Mani, B. Lane, A. Donmez, S. Feng, S. Moylan, and R. Fesperman, "Measurement science needs for real-time control of additive manufacturing powder bed fusion processes," U.S. Dept. Commerce, Nat. Inst. Standards Technol., Gaithersburg, MD, USA, Tech. Rep. NISTIR 8036, 2015.
- [33] N. Shamsaei, A. Yadollahi, L. Bian, and S. M. Thompson, "An overview of direct laser deposition for additive manufacturing; Part II: Mechanical behavior, process parameter optimization and control," *Addit. Manuf.*, vol. 8, pp. 12–35, Oct. 2015.
- [34] R. B. Dinwiddie, L. J. Love, and J. C. Rowe, "Real-time process monitoring and temperature mapping of a 3D polymer printing process," *Proc. SPIE*, vol. 8705, p. 87050L, May 2013.
- [35] C. Kousiatza and D. Karalekas, "In-situ monitoring of strain and temperature distributions during fused deposition modeling process," *Mater. Des.*, vol. 97, pp. 400–406, May 2016.
- [36] Y. Tlegenov, Y. S. Wong, and G. S. Hong, "A dynamic model for nozzle clog monitoring in fused deposition modelling," *Rapid Prototyping J.*, vol. 23, no. 2, pp. 391–400, 2017.
- [37] H. Wu, Y. Wang, and Z. Yu, "In situ monitoring of FDM machine condition via acoustic emission," *Int. J. Adv. Manuf. Technol.*, vol. 84, nos. 5–8, pp. 1483–1495, 2016.
- [38] K. Tong, S. Joshi, and E. A. Lehtihet, "Error compensation for fused deposition modeling (FDM) machine by correcting slice files," *Rapid Prototyping J.*, vol. 14, no. 1, pp. 4–14, 2008.
- [39] Q. Huang, H. Nouri, K. Xu, Y. Chen, S. Sosina, and T. Dasgupta, "Statistical predictive modeling and compensation of geometric deviations of three-dimensional printed products," *J. Manuf. Sci. Eng.*, vol. 136, no. 6, p. 061008, 2014.
- [40] A. Wang, S. Song, Q. Huang, and F. Tsung, "In-plane shape-deviation modeling and compensation for fused deposition modeling processes," *IEEE Trans. Autom. Sci. Eng.*, vol. 14, no. 2, pp. 968–976, Apr. 2017.
- [41] I. Olkin and R. F. Tate, "Multivariate correlation models with mixed discrete and continuous variables," *Ann. Math. Stat.*, vol. 32, no. 2, pp. 448–465, 1961.
- [42] D. R. Cox and N. Wermuth, "Response models for mixed binary and quantitative variables," *Biometrika*, vol. 79, no. 3, pp. 441–461, 1992.
- [43] G. M. Fitzmaurice and N. M. Laird, "Regression models for mixed discrete and continuous responses with potentially missing values," *Biometrics*, vol. 53, no. 1, pp. 110–122, 1997.
- [44] J. Shi, *Stream of Variation Modeling and Analysis for Multistage Manufacturing Processes*. Boca Raton, FL, USA: CRC Press, 2006.
- [45] K. Wang and F. Tsung, "Run-to-run process adjustment using categorical observations," *J. Quality Technol.*, vol. 39, no. 4, pp. 312–325, 2007.
- [46] K. Liu and S. Huang, "Integration of data fusion methodology and degradation modeling process to improve prognostics," *IEEE Trans. Autom. Sci. Eng.*, vol. 13, no. 1, pp. 344–354, Jan. 2016.
- [47] S. Zhou, N. Jin, and J. Jin, "Cycle-based signal monitoring using a directionally variant multivariate control chart system," *IIE Trans.*, vol. 37, no. 11, pp. 971–982, 2005.
- [48] C. Cheng *et al.*, "Time series forecasting for nonlinear and non-stationary processes: A review and comparative study," *IIE Trans.*, vol. 47, no. 10, pp. 1053–1071, 2015.
- [49] R. F. Tate, "Correlation between a discrete and a continuous variable. Point-biserial correlation," *Ann. Math. Stat.*, vol. 25, no. 3, pp. 603–607, 1954.
- [50] P. J. Catalano and L. M. Ryan, "Bivariate latent variable models for clustered discrete and continuous outcomes," *J. Amer. Stat. Assoc.*, vol. 87, no. 419, pp. 651–658, 1992.
- [51] G. M. Fitzmaurice and N. M. Laird, "Regression models for a bivariate discrete and continuous outcome with clustering," *J. Amer. Stat. Assoc.*, vol. 90, no. 431, pp. 845–852, 1995.
- [52] J. O. Ramsay and B. W. Silverman, *Functional Data Analysis*. New York, NY, USA: Springer, 2005.
- [53] M. Yuan and Y. Lin, "Model selection and estimation in regression with grouped variables," *J. Roy. Stat. Soc., B (Stat. Methodol.)*, vol. 68, no. 1, pp. 49–67, 2006.
- [54] T. Hastie, R. Tibshirani, and M. Wainwright, *Statistical Learning With Sparsity: The Lasso and Generalizations*. Boca Raton, FL, USA: CRC Press, 2015.
- [55] L. Breiman, "Better subset regression using the nonnegative garrote," *Technometrics*, vol. 37, no. 4, pp. 373–384, 1995.
- [56] T. Hastie, R. Tibshirani, and J. H. Friedman, *The Elements of Statistical Learning: Data Mining, Inference, and Prediction*. New York, NY, USA: Springer, 2009.
- [57] J. Friedman, T. Hastie, and R. Tibshirani, "Regularization paths for generalized linear models via coordinate descent," *J. Stat. Softw.*, vol. 33, no. 1, pp. 1–22, 2010.
- [58] N. Tandon and A. Choudhury, "A review of vibration and acoustic measurement methods for the detection of defects in rolling element bearings," *Tribol. Int.*, vol. 32, no. 8, pp. 469–480, 1999.
- [59] W. H. Woodall, "Control charts based on attribute data: Bibliography and review," *J. Quality Technol.*, vol. 29, no. 2, pp. 172–183, 1997.

- [60] S. H. Steiner, R. J. Cook, V. T. Farewell, and T. Treasure, "Monitoring surgical performance using risk-adjusted cumulative sum charts," *Biostatistics*, vol. 1, no. 4, pp. 441–452, 2000.
- [61] V. R. Joseph, "Robust parameter design with feed-forward control," *Technometrics*, vol. 45, no. 4, pp. 284–292, 2003.

Hongyue Sun (M'17) received the B.E. degree in mechanical engineering and automation from the Beijing Institute of Technology, Beijing, China, in 2012, the M.S. degree in statistics, and the Ph.D. degree in industrial engineering from Virginia Tech, Blacksburg, VA, USA, in 2015 and 2017, respectively.

He is an Assistant Professor with the Department of Industrial and Systems Engineering, University at Buffalo, Buffalo, NY, USA. His research is on data analytics for advanced manufacturing processes and energy systems.

Prof. Sun is a member of the Institute for Operations Research and the Management Sciences, the Institute of Industrial and Systems Engineers, and the American Society of Mechanical Engineers.

Prahalad K. Rao received the B.Eng. degree (First Class) from Victoria Jubilee Technical Institute, Bombay University, Mumbai, India, in 2003, and the M.S. and Ph.D. degrees from the School of Industrial Engineering and Management, Oklahoma State University, Stillwater, OK, USA, in 2006 and 2013, respectively.

He is currently an Assistant Professor with the Department of Mechanical and Materials Engineering, University of Nebraska–Lincoln, Lincoln, NE, USA. His research focused on sensor-based monitoring of manufacturing processes—ultraprecision diamond turning, chemical mechanical planarization, and additive manufacturing processes.

Prof. Rao is a member of the Institute of Industrial and Systems Engineers, the American Society for Quality, and the Institute for Operations Research and the Management Sciences. He received the Alpha Pi Mu Outstanding Research Assistant Award by OSU in 2008. He is an amateur radio ARRL General Class licensee with the call sign K5RAO.

Zhenyu (James) Kong (M'17) received the B.S. and M.S. degrees in mechanical engineering from the Harbin Institute of Technology, Harbin, China, in 1993 and 1995, respectively, and the Ph.D. degree from the Department of Industrial and Systems Engineering, University of Wisconsin–Madison, Madison, WI, USA, in 2004.

He was a Faculty Member of the School of Industrial Engineering and Management, Oklahoma State University, Stillwater, OK, USA. He is currently an Associate Professor with the Grado Department of Industrial and Systems Engineering, Virginia Tech, Blacksburg, VA, USA. His research is sponsored by the National Science Foundation, the Department of Transportation, the Commonwealth Center for Advanced Manufacturing, and Dimensional Control Systems Inc. His research focuses on automatic quality control for large and complex manufacturing processes/systems.

Prof. Kong is a member of the Institute of Industrial and Systems Engineers, the Institute for Operations Research and the Management Sciences, and the American Society of Mechanical Engineers.

Xinwei Deng received the bachelor's degree in mathematics from Nanjing University, Nanjing, China, and the Ph.D. degree in industrial engineering from Georgia Tech, Atlanta, GA, USA.

He is an Associate Professor with the Department of Statistics, Virginia Tech, Blacksburg, VA, USA. His research interests include statistical modeling and analysis of massive data, including high-dimensional classification, graphical model estimation, interface between experimental design and machine learning, and statistical approaches to nanotechnology.

Prof. Deng is a member of the the Institute for Operations Research and the Management Sciences and the American Standards Association.

Ran Jin (M'17) received the bachelor's degree in electronic engineering from Tsinghua University, Beijing, China, the master's degrees in industrial engineering and in statistics from the University of Michigan, Ann Arbor, MI, USA, and the Ph.D. degree in industrial engineering from Georgia Tech, Atlanta, GA, USA.

He is an Assistant Professor with the Grado Department of Industrial and Systems Engineering at Virginia Tech, Blacksburg, VA, USA. His research interests include engineering driven data fusion for manufacturing system modeling and performance improvements, such as the integration of data mining methods and engineering domain knowledge for multistage system modeling and variation reduction, and sensing, modeling, and optimization based on spatial correlated responses.

Prof. Jin is a member of the Institute for Operations Research and the Management Sciences, the Institute of Industrial and Systems Engineers, and the American Society of Mechanical Engineers.